The Valence Electronic Charge Densities of Si and Ge and the Effect of Core-Orthogonalization

Bull. Coll. Med. Sci. Tohoku Univ. 1 : 15~26, 1992

The Valence Electronic Charge Densities of Si and Ge and the Effect of Core-Orthogonalization

Teiji KOBAYASI and Hisashi NARA*

General Education, College of Medical Sciences, Tohoku University

**Education Center for Information Processing, Tohoku University*

Key words: Pseudopotential theory, Core-orthogonalization, Semiconductor, Valence band, Charge density

Electronic charge densities of Si and Ge are calculated by using nonlocal pseudopotential method. For Si, the density is calculated beyond the approximation of pseudoelectron by introducing the core-orthogonalization of the wave function of valence electron. The result is compared with the charge density constructed by using experimental X-ray structure factors up to high Miller indices. The shape of the experimental bond is strongly elongated along the bond-axis. The theory gives a nearly spherical shape. Although the nonlocality and the orthogonalization tend to improve the density, the discrepancy in the shape is not removed. Possible sources of the discrepancy are discussed.

Introduction

Energy band structures of valence bands of fundamental IV, III-V and II-VI semiconductors are known in detail, mainly through pseudopotential calculations.[1] Charge density of the valence electrons corresponding to the spatial distribution of the electrons is one of important information on the valence states. The Fourier components of the charge density are related directly to X-ray structure factors. Charge density is also a probe for a quality of the wave functions and/or of the potentials used in calculating energy band.

Yang and Coppens[2] calculated the valence electronic charge density of Si using very accurate experimental data of X-ray structure factors collected from various available sources. The resulting charge density shows a distribution of valence electrons of a clearly covalent nature. The shape of the equidensity contours of the covalent bond is strongly elongated to the bonding direction of Si-Si bond.

Chelikowsky and Cohen[3] calculated the valence charge density of Si using pseudopotential method and compared it with Yang-Coppens' *experimental* result. The maximum value of the calculated density at the center of bond is in fairly good agreement with Yang-Coppens' result, in both cases of local and nonlocal pseudopotentials. The charge density calculated using the nonlocal pseudopotential shows a shape of the bond slightly elongated to the bonding direction, while for the local potential it is rather expanded perpendicular to the bonding direction. Walter and Cohen's local pseudopotential approach[4] also gives a similar result. These theoretical charge densities show nearly spherical distribution of valence electrons around the center of bond, so that

there is a considerable discrepancy for the shape of the bond between the theory and the experiment.

In constructing the *experimental* charge density, Yang and Coppens adopted many experimental X-ray structure factors with Miller indices up to (880). We will point out, in § 4, that the strongly elongated shape of the bond experimentally obtained is caused by the X-ray structure factors with higher Miller indices from (751) to (880).

In order to investigate theoretically the contribution of higher components to the shape of the bond, it is necessary to calculate the *true* wave functions of valence electrons beyond the pseudowave functions, if the pseudowave functions themselves can be obtained in a sufficient accuracy. Here we define a pseudovalence electron as an electron moving in a weakened pseudopotential field, which is described by a pseudowave function, namely, the so-called smooth part of the true wave function.

In the framework of the pseudopotential theory, this is attained by introducing the core-orthogonalization into the valence electronic states. An approximate true wave function of valence electron can be obtained by orthogonalizing the pseudowave function to the wave functions of core electrons, which can be described by the tight binding approximation. The orthogonalized wave function shows a spatially rapid oscillation in the vicinity of atoms. This localized oscillation introduces high-momentum components into the wave function and improves the electronic structure in the momentum space. As a result, higher Fourier components of charge density are much improved. Naturally, the electron density around the atoms is largely affected by the orthogonalization. It is very interesting to see to what extent the electron distribution is affected in the region of bond.

A nonlocality of pseudopotential also play an important role on electron distribution, because a repulsive nature of the pseudopotential depends on the symmetry and/or on the energy level of electronic state.

In this paper, we calculate valence electron X-ray structure factors up to very high Miller indices by using local and nonlocal pseudopotentials, and construct the charge densities of pseudo- (Si and Ge) and true- (Si) valence electrons. The results are compared with experimental X-ray structure factors and Yang-Coppens' map of charge density. Effects of nonlocality of pseudopotential and core-orthogonalization are discussed, especially in connection with the shape of the bond. The shape of the theoretical bond is nearly shperical. In § 2 we perform the calculation of Fourier components of the valence electron density, and construct the map of the density, and the results are given in § 3. Section 4 is devoted to analysis of the results and discussion.

Method of Calculation

The valence electron density $\rho(\boldsymbol{r})$ is defined as

$$\rho(\boldsymbol{r})=2\sum_{n}\sum_{\boldsymbol{k}}|\Psi_{n\boldsymbol{k}}(\boldsymbol{r})|^{2}, \qquad (1)$$

where $\Psi_{n\boldsymbol{k}}$ is the wave function of the valence electron with wave vector $\boldsymbol{k}$ in the n-th valence band. The summations are taken over the occupied states. The charge density is $e\rho(\boldsymbol{r})$, where e is the electron charge. If the pseudowave function $\Phi_{n\boldsymbol{k}}$ is adopted as $\Psi_{n\boldsymbol{k}}$, $\rho(\boldsymbol{r})$ gives the pseudovalence electron density $\rho_{\mathrm{pv}}(\boldsymbol{r})$. In the pseudopotential framework, the true valence electron density $\rho_{\mathrm{v}}(\boldsymbol{r})$ is given by eq. (1) by using the function orthogonalized to the core functions $\Psi_{c\boldsymbol{k}}$'s;

$$\Psi_{nk}(\boldsymbol{r})=N_{nk}[\Phi_{nk}(\boldsymbol{r})-\sum_{c}<\Psi_{ck}|\Phi_{nk}>\Psi_{ck}(\boldsymbol{r})], \tag{2}$$

where N_{nk} is a normalization constant. We approximate Ψ_{ck} by the Bloch sum of the ionic core orbitals.

The pseudowave function Φ_{nk} is expanded in terms of plane waves as

$$\Phi_{nk}(\boldsymbol{r})=\sum_{G}C_{nk}(\boldsymbol{G})\exp[i(\boldsymbol{k}+\boldsymbol{G})\cdot\boldsymbol{r}]/\sqrt{\Omega}, \tag{3}$$

where $\boldsymbol{G}$ is the reciprocal lattice vector and Ω is the crystal volume. The coefficients C_{nk}'s are obtained in the energy band calculation. The local part of the pseudopotential is described by the parameters of potential form factors $V(\boldsymbol{G})$'s. The nonlocal part of our pseudopotential is of Abarenkov-Heine form,[5] $V_{NL}(\boldsymbol{r})=\sum_{l}A_l\Theta_l(R_l-r)P_l$, with the parameters of well depth A_l and well radius R_l, where P_l is a projection operator and l is an angular momentum quantum number. The l-component of valence states feels energy-dependent potential through the $\boldsymbol{k}$-dependent matrix elements of $V_{NL}(\boldsymbol{r})$. For Si and Ge, various sets of parameters are previously determined[6] so as to reproduce various energy differences taken from optical, UPS and XPS data over the energy range of about 20 eV above the bottom of the valence bands. The relative rms deviations δ's of the level fitting are 7 (Si)~10 (Ge)% and 3~4% (Si and Ge) for the local and the nonlocal pseudopotentials, respectively. The nonlocality, therefore, appreciably improves the quality of energy band for Si, as well as for Ge. Values of parameters are listed in Table I, together with δ's and the lattice constants a's. The notation, for example, 3L+NL (p) means the potential optimized with three local and p-($l=1$) nonlocal parameters. All plane waves with reciprocal lattice vectors $\boldsymbol{G}$ satisfying $(\boldsymbol{k}+\boldsymbol{G})^2-\boldsymbol{k}^2\leqq 20\,(2\pi/a)^2$ are adopted in expanding Φ_{nk}.

Table I. Local and nonlocal parameters of pseudopotentials of Si and Ge.

		Si		Ge
		3L	3L+NL(p)	3L+NL(d)
$V(111)$		−0.2247	−0.2053	−0.2422
$V(220)$	(Ry)	0.0544	0.0355	0.0255
$V(311)$		0.0767	0.0724	0.0526
A_1	(Ry)		−1.039†	
R_1	(a.u.)		1.25†	
A_2	(Ry)			83.77†
R_2	(a.u.)			0.98†
δ	(%)	6.70	3.82	2.96
a	(a.u.)	10.26		10.70

† Notice the magnitudes of A_l and R_l. If potential parameters are optimized in a fully interdependent way, a good quality of energy band can be attained over a wide range of parameters A_l and R_l.[6]

We calculate the Fourier transform $\rho(\boldsymbol{G})$ of the electron density,

$$\rho(\boldsymbol{G})=\frac{1}{\Omega}\int\rho(\boldsymbol{r})\exp(-i\boldsymbol{G}\cdot\boldsymbol{r})\,d^3\boldsymbol{r}, \tag{4}$$

and construct $\rho(\boldsymbol{r})$ by

$$\rho(\boldsymbol{r})=\sum_{G}\rho(\boldsymbol{G})\exp(i\boldsymbol{G}\cdot\boldsymbol{r}). \tag{5}$$

From the definition of the X-ray structure factor;

$$F(\boldsymbol{G})=\int_{\text{unit cell}}\rho(\boldsymbol{r})\exp(-i\boldsymbol{G}\cdot\boldsymbol{r})\,d^3\boldsymbol{r}, \tag{6}$$

we have

$$F(\boldsymbol{G})=\Omega_0\rho(\boldsymbol{G}), \tag{7}$$

where Ω_0 is the unit cell volume.

As mentioned in § 1, in order to obtain more accurate higher Fourier component $\rho(\boldsymbol{G})$, we calculate for Si not only the pseudo- but also

the true-valence electron densities. The Roothaan-Hatree-Fock wave functions calculated by Clementi[7] are used for 1s, 2s and 2p core orbitals of Si^{4+} in the Bloch sums Ψ_{ck}'s. The orthogonalized wave function Ψ_{nk} is also expanded in terms of plane waves as

$$\Psi_{nk}(\boldsymbol{r})=\sum_{G}\tilde{C}_{nk}(\boldsymbol{G})\exp[i(\boldsymbol{k}+\boldsymbol{G})\cdot\boldsymbol{r}]/\sqrt{\Omega}. \quad (8)$$

Because of the high localization of the core orbitals, the Fourier expansion of eq. (8) was forced to include a sufficiently high reciprocal lattice vectors up to the group of $\boldsymbol{G}$ (13, 7, 7).

In Ge, the core-orthogonalization effect is expected to be more important, because of the shallower 3d-core states. The true valence electron density $\rho_v(\boldsymbol{r})$ of Ge will be treated in a separated paper.

Results of Calculation

The results of $\rho_{pv}(\boldsymbol{G})$ of Si and Ge are given in Table II, in units of $1/\Omega_0$, where $\Omega_0=a^3/4$. In Table III, $\rho_v(\boldsymbol{G})$'s for Si calculated by using the 3L+NL (p) potential are given together with the valence electron X-ray structure factors, $F_v(\boldsymbol{G})$'s, deduced from the experimental data adopted by Yang and Coppens.[2] The $F_v(\boldsymbol{G})$'s are obtained from the experimental structure factors by correcting core contributions, calculated by Fukamachi[8] using the Roothaan-Hatree-Fock atomic wave functions,[7] with additional corrections for the effects of scattering of core electrons and of thermal smearing. Equation (7) makes it possible to compare $\rho_v(\boldsymbol{G})$ in units of $1/\Omega_0$ directly with $F_v(\boldsymbol{G})$. The values of $\rho_{pv}(\boldsymbol{G})$ are negligibly small for $\boldsymbol{G}$'s larger than $\boldsymbol{G}$ (622) and are not listed in Table II.

Figures 1, 2 and 3 show the maps of pseudovalence electron densities $\rho_{pv}(\boldsymbol{r})$ in the

Table II. Fourier components of the pseudovalence electron densities, $\rho_{pv}(\boldsymbol{G})$, of Si and Ge, in units of $1/\Omega_0$. Potentials used in the energy band calculation are shown by the symbols.

	Si		Ge
$\boldsymbol{G}$	3L	3L+NL(p)	3L+NL(d)
000	8.0	8.0	8.0
111	−1.6627	−1.7046	−1.8332
220	0.3115	0.1981	0.0961
311	0.4732	0.4213	0.3543
222	0.5261	0.4895	0.4348
400	0.2547	0.2662	0.2275
331	0.0285	0.0176	0.0056
422	−0.0022	−0.0284	−0.0204
333	0.0055	−0.0217	−0.0012
511	0.0015	−0.0147	−0.0105
440	0.0237	0.0121	0.0089
531	0.0123	0.0049	0.0060
442	0.0099	0.0036	0.0081
620	0.0061	0.0025	0.0029
533	0.0029	0.0021	0.0020
622	0.0025	0.0021	0.0017

$(1\bar{1}0)$ plane containing the bonds calculated by using the Si 3L, Si 3L+NL (p) and Ge 3L+NL (d), respectively. Figure 4 shows the map of the true valence electron density $\rho_v(\boldsymbol{r})$ of Si calculated by using 3L+NL (p) potential. The maximum values of $\rho_{pv}(\boldsymbol{r})$ at the center of bond are $27.06/\Omega_0$ [Si, 3L], $26.21/\Omega_0$ [Si, 3L+NL (p)] and $24.94/\Omega_0$ [Ge, 3L+NL (d)]. The $\rho_v(\boldsymbol{r})$ of Si gives the maximum density of $26.84/\Omega_0$.

In Fig. 5, the true valence electron density $\rho_v(\boldsymbol{r})$ is compared with the pseudovalence electron density $\rho_{pv}(\boldsymbol{r})$ along the bonding direction.

In the following section, effects of the nonlocality of the potential and the core-orthogonalization on the charge density distribution are discussed, and a possible origin of the strongly elongated shape of the bond observed in the Yang-Coppens' density map of Si is

Table III. Fourier components of the true valence electron density $\rho_v(\boldsymbol{G})$ of Si and the experimental X-ray structure factors $F_v(\boldsymbol{G})$ deduced from the data given in ref. 2, in units of $1/\Omega_0$. The axial ratio of the equidensity contour of bond A/B is given as a function of truncating $\boldsymbol{G}$ in $\boldsymbol{G}$-summation of eq. (5).

	3L+NL(p)		Experiment			3L+NL(p)		Experiment	
$\boldsymbol{G}$	$\rho_v(\boldsymbol{G})$	A/B	$F_v(\boldsymbol{G})$	A/B	$\boldsymbol{G}$	$\rho_v(\boldsymbol{G})$	A/B	$F_v(\boldsymbol{G})$	A/B
000	8.0		8.0		733	−0.0218	0.981	—	
111	−1.6375		−1.7650		644	−0.0018	0.987	—	
220	0.2896		0.0987		660	−0.0274	1.085	−0.0627	1.74
311	0.4706	0.684	0.3715	0.89	822	−0.0276	1.110	−0.0627	1.80
222	0.4970	0.783	0.3498	0.92	751	−0.0188	1.379	−0.0285	2.73
400	0.2920	0.817	0.4118	0.94	555	0.0172	1.306	0.0285	2.54
331	0.0127	0.823	−0.0809	0.90	662	−0.0009	1.310	—	
422	−0.0161	0.834	−0.1065	1.02	840	−0.0240	1.521	—	
333	−0.0047	0.838	−0.0921	1.14	753	0.0153	1.176	—	
511	−0.0008	0.839	−0.0797	1.25	911	−0.0161	1.203	—	
440	0.0408	0.851	−0.0345	1.28	842	−0.0006	1.216	—	
531	0.0283	0.816	0.0701	1.00	664	0.0205	1.005	—	
442	0.0067	0.802	0.0100	0.97	931	−0.0139	1.102	—	
620	0.0372	0.747	−0.0775	1.15	844	0.0173	1.075	0.0041	2.43
533	−0.0205	0.762	0.0467	1.05	755	0.0121	1.009	—	
622	0.0036	0.766	—		771	0.0113	1.048	—	
444	−0.0346	0.752	−0.0575	1.05	933	0.0112	0.998	—	
551	−0.0242	0.824	−0.1876	1.64	⋮			⋮	
711	0.0258	0.814	0.1876	1.23	⋮			⋮	
642	−0.0338	0.925	−0.0730	1.49	880	0.0073	0.779	0.0040	2.36
731	−0.0228	0.870	—		⋮			⋮	
553	−0.0246	0.869	—		⋮			⋮	
800	0.0312	0.877	—		1377	0.0019	0.895	—	

analyzed on the basis of our theoretical results.

Discussion

As seen from $\rho_{pv}(\boldsymbol{G})$'s in Table II and $\rho_v(\boldsymbol{G})$'s in Table III for Si, the Fourier components of electron density are significantly improved by introducing the nonlocality of pseudopotential and the core-orthogonalization. The core-orthogonalization improves the rapidly decreasing nature of $\rho_{pv}(\boldsymbol{G})$ especially for large $\boldsymbol{G}$'s, as expected. However, the resulting $\rho_v(\boldsymbol{G})$'s are considerably smaller than the experimental $F_v(\boldsymbol{G})$'s in their magnitudes.

The maximum density $26.84/\Omega_0$ of $\rho_v(\boldsymbol{r})$ for Si at the center of bond is larger than $26.21/\Omega_0$ of the 3L+NL (p) $\rho_{pv}(\boldsymbol{r})$, both in good agreement with Yang-Coppens' experimental result of about $28/\Omega_0$. The maximum value $27.06/\Omega_0$ of the 3L $\rho_{pv}(\boldsymbol{r})$ is closer to the experimental value, but the quality of the energy band is not so good, as mentioned in § 2.[5)6)] Our maximum values of $\rho_{pv}(\boldsymbol{r})$ are also close to those of Chelikowsky-Cohen for Si[3)] and Ge[9)], and of Walter-Cohen for Si.[4)]

The equidensity contours of the 3L $\rho_{pv}(\boldsymbol{r})$ of Si expand perpendicular to the bonding direc-

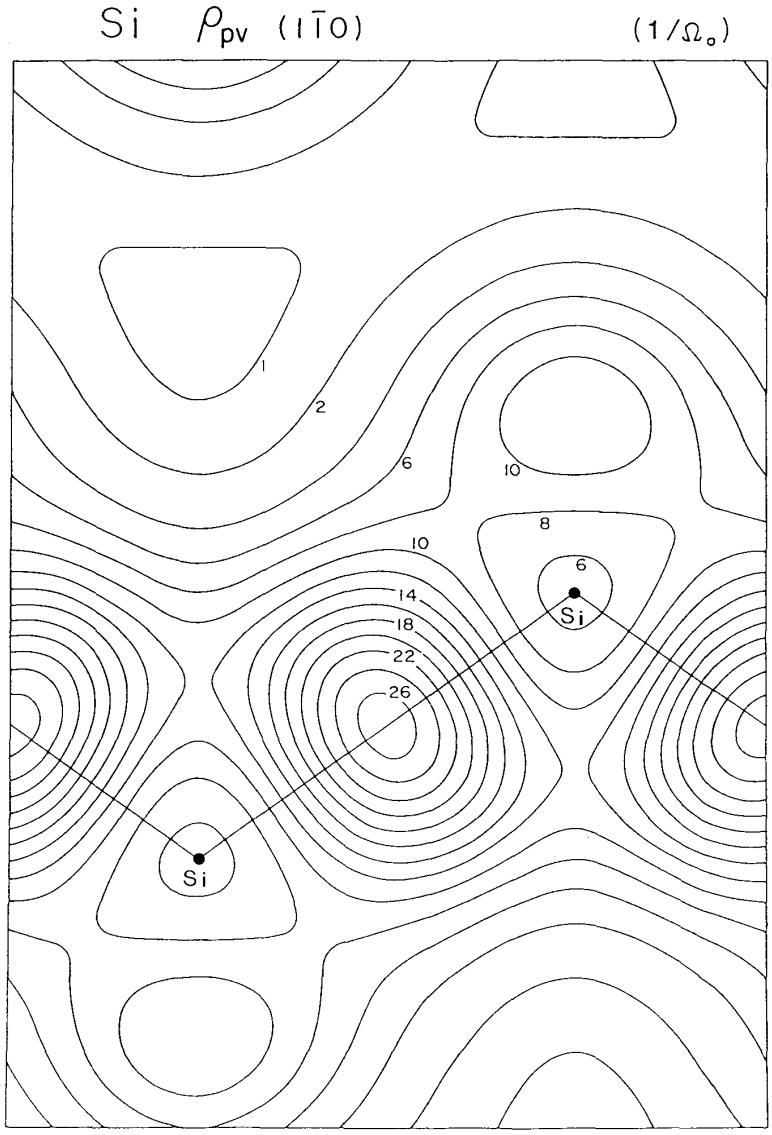

Fig. 1. Pseudovalence electron density of Si in the $(1\bar{1}0)$ plane calculated by using the 3L pseudopotential, in units of $1/\Omega_0$.

tion, as shown in Fig. 1. Chelikowsky-Cohen's[3] and Walter-Cohen's[4] local potential results show a similar aspect of the shape. Figure 2 shows that under the nonlocal 3L+NL(p) pseudopotential the bonding electrons spread slightly toward the atom sites. This is caused by the potential becoming less repulsive on p-components of valence states. [It should be noticed that an influence of introducing the nonlocal part NL (l) to the nL-type local potential is not necessarily confined to the l-component of valence states, because our local part of the nL+NL (l) potential is not the same with the nL local potential.] Chelikowsky-Cohen's nonlocal result[3] for Si shows a weak elongation to the bonding direction. Our result for Ge gives a not elongated but very spherical bond (see Fig. 3).

Being orthogonalized to the 1s-, 2s- and 2p-core states, the true valence electron shows approximately atomic behaviours around the Si atom. An electron pile-up of these atom-like

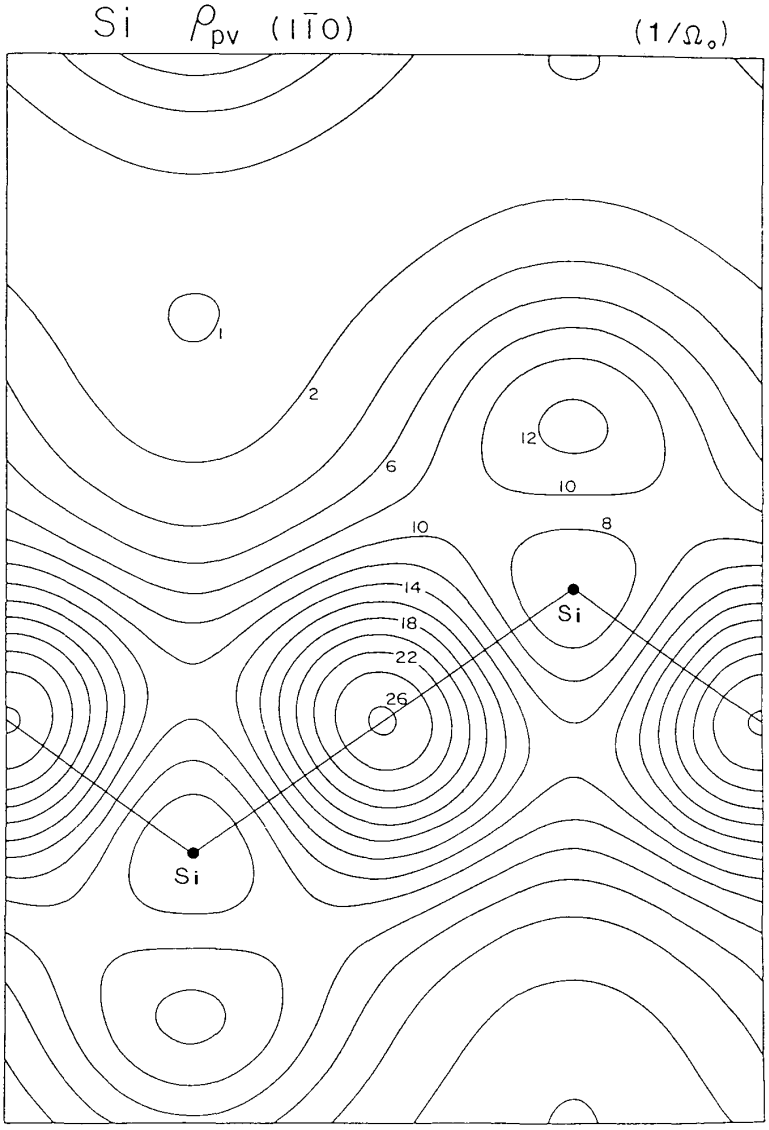

Fig. 2. Pseudovalence electron density of Si in the (1$\bar{1}$0) plane calculated by using the 3L+NL(p) pseudopotential, in units of $1/\Omega_0$.

components makes a peak of density around the atom, as shown in Figs. 4 and 5. Since the peak is composed of electrons transfered from the region of bond, the covalent bond peak is slightly sharpened as indicated by the dashed line in Fig. 5. The core-orthogonalization gives a small increase of 2.4% of the density at the center of bond.

Figure 6 shows the charge density map of valence electrons of Si constructed from the experimental X-ray structure factors $F_v(\boldsymbol{G})$'s given in Table III, where $F_v(\boldsymbol{G})$'s are reduced to the quantity of electron density for a direct comparison with $\rho_v(\boldsymbol{G})$'s. The map corresponds to the Yang-Coppens' original[2], but is reconstructed by removing some inconsistencies with the crystalline symmetry. Comparison with Fig. 4 shows that the distribution of electrons around the atom reflects the effect of core-orthogonalization.

We notice, however, the equidensity contours around the center of bond being extremely

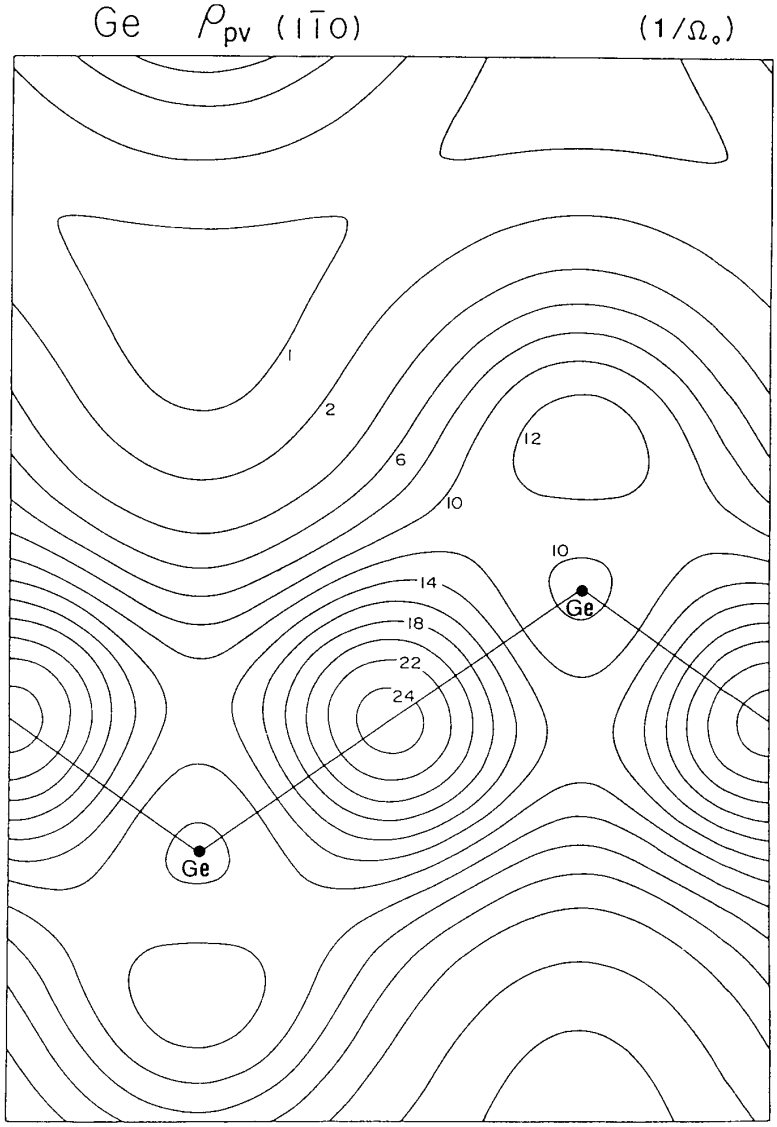

Fig. 3. Pseudovalence electron density of Ge in the (1$\bar{1}$0) plane calculated by using the 3L+NL(d) pseudopotential, in units of $1/\Omega_0$.

elongated to the bonding direction. In contrast to the experimental shape of the bond, the calculated ones are spherical. The slightly elongated Chelikowsky-Cohen's result[3] also seems nearly spherical.

In order to resolve an origin of the strong elongation of the experimental shape of the bond, we analyze the shape as a function of a truncation in the $\boldsymbol{G}$-summation of eq. (5), in which the experimental $F_v(\boldsymbol{G})$'s are used for $\rho_v(\boldsymbol{G})$'s. As can be seen in Fig. 6, the equidensity contour in the vicinity of the center of bond can be approximated by an ellipse. We define A and B as axial radius lengths of the ellipse along and perpendicular to the bonding direction, respectively. If the axial ratio A/B is larger than unity, the bond is elongated toward the bonding direction. The ratio varies with the truncating vector $\boldsymbol{G}_c$ in the $\boldsymbol{G}$-summation. Of course, all relevant $\boldsymbol{G}$'s in the group of the truncating $\boldsymbol{G}_c$ should be taken into the summation to keep the symmetry of the crystal. The

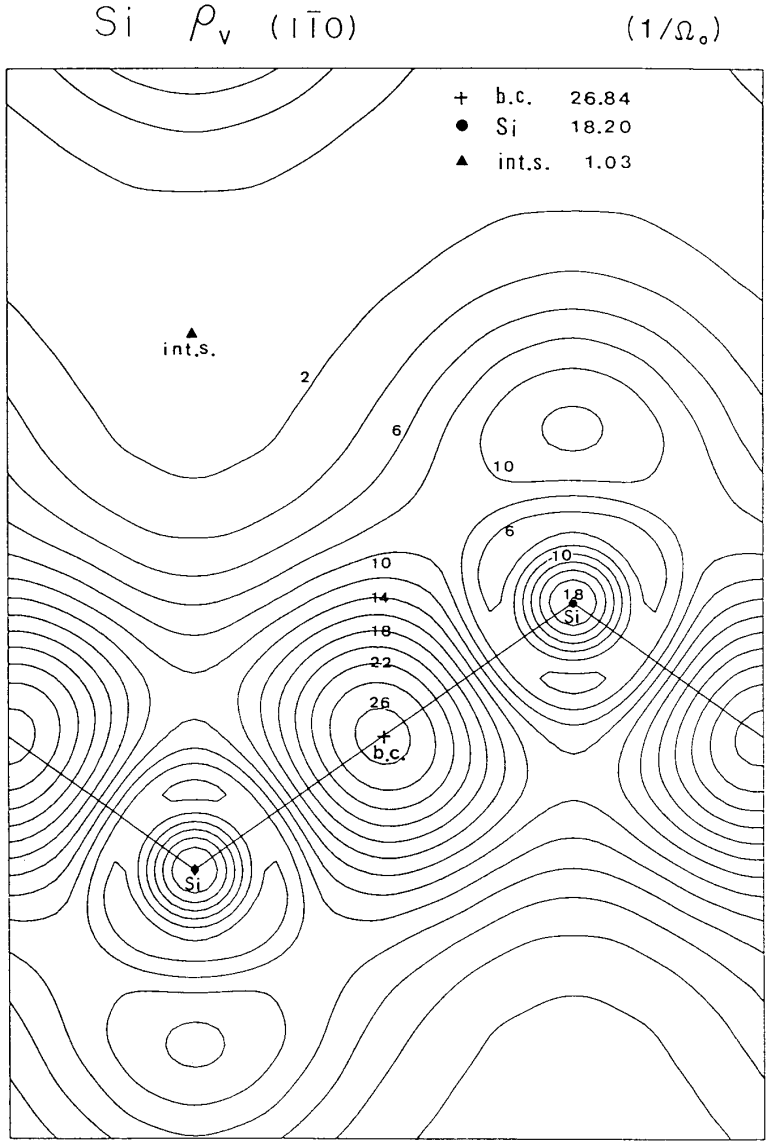

Fig. 4. *True* valence electron density of Si in the (1$\bar{1}$0) plane calculated by using the 3L+NL(p) pseudopotential and taking the 1s-, 2s- and 2p-core-orthogonalizations into account, in units of $1/\Omega_0$.

same analysis is made for our theoretical map of $\rho_v(\boldsymbol{r})$ shown in Fig. 4. The results are listed in Table III.

Before comparing the two sets of A/B's, two marked features in the experimental $F_v(\boldsymbol{G})$'s given in Table III should be noticed: (1) $F_v(\boldsymbol{G})$'s for higher $\boldsymbol{G}$ are generally much larger than the corresponding theoretical $\rho_v(\boldsymbol{G})$'s. (2) Because of the lack of available data, the experimental $F_v(\boldsymbol{G})$'s are not used for many higher G's in constructing Yang-Coppens' density map, which are indicated by bar in Table III. On the analogy of $\rho_v(\boldsymbol{G})$, the lacked data of $F_v(\boldsymbol{G})$ may be of an order in magnitude similar to the available data; namely, they may be generally larger than theoretical ones.

From the results of the ratio A/B's given in Table III, the strong elongation of the experimental bond shape is quantitatively obvious. The experimental A/B increases abruptly as

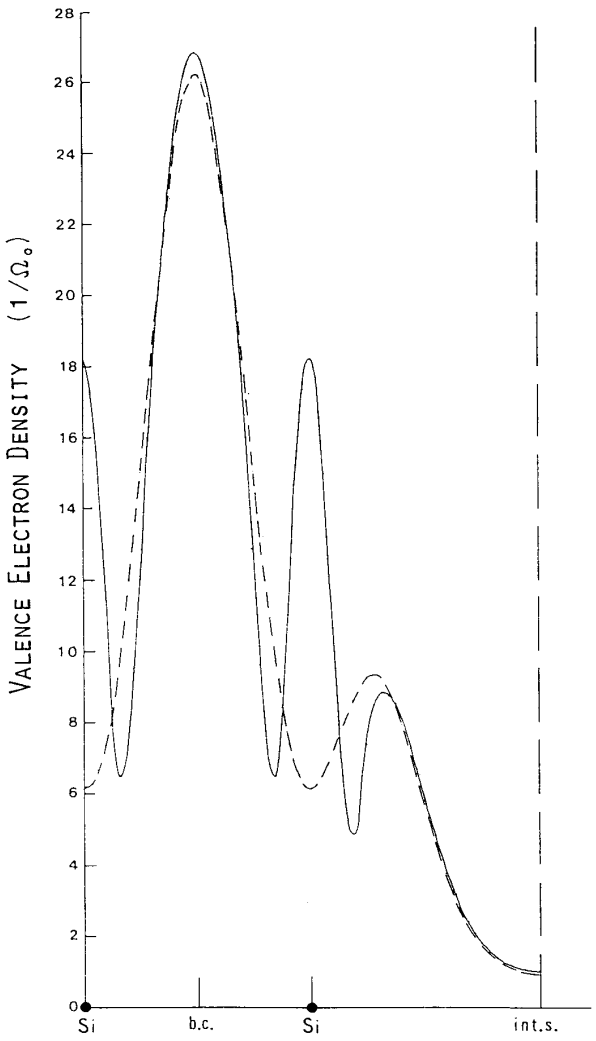

Fig. 5. The true valence electron density (——) and the pseudovalence electron density (- - -) of Si along the direction of Si-Si bond, in units of $1/\Omega_0$.

$\boldsymbol{G}_c$ passes $\boldsymbol{G}$ (551), $\boldsymbol{G}$ (660) and $\boldsymbol{G}$ (751), and it exceeds the value 2. On the other hand, the theoretical one varies rather continuously. It becomes larger than unity at $\boldsymbol{G}$ (660) and gradually increases to 1.52 at $\boldsymbol{G}$ (840) with increments parallel to but smaller than those in the experimental A/B's. Toward the $\boldsymbol{G}$'s higher than $\boldsymbol{G}$ (840), however, the ratio decreases gradually and is settled to the value of 0.8~0.9, showing an ellipse slightly compressed along the bonding direction. The contribution of the component ρ_v (753) is especially significant to decrease the theoretical value of A/B. Further contributions from the $\boldsymbol{G}$'s larger than $\boldsymbol{G}$ (840) makes A/B smaller than unity.

Because of the lack of the corresponding F_v (840), however, such a cancelling contributions are not introduced in the the Yang-Coppens' result. This fact seems to be the most serious origin of the extreme elongation of the bond observed in the Yang-Coppens' density map. In this meaning, a large part of the strong elongation is considered to be possibly unphysical.

In order to make a physical reason of elongation clearer, it is necessary to account for the considerable differences in magnitude between the experimental and the theoretical X-ray structure factors with high Miller indices. As seen from the results given in Tables II and III, a nonlocality of pseudopotential and the core-orthogonalization effect are essential in improving the charge density distribution. At the present stage of the pseudopotential theory, however, a physical effect of such a strong elongation can not be expected quantitatively.

In Ge, the core-orthogonalization effect is more important because of the shallower 3d-core states. We are now evaluating the effect of the 3d-core orthogonalization on the charge and the momentum density distributions. The latter can be compared with experimental results of ACAR (angular correlation of positron annihilation radiations) spectra of the positron annihilation and the Compton scattering profiles.

Acknowledgments

The authors would like to thank Professor N. Kato of Meijo University, Professor R. Uno of Nihon University and Dr. O. Terasaki of Tohoku University for discussions.

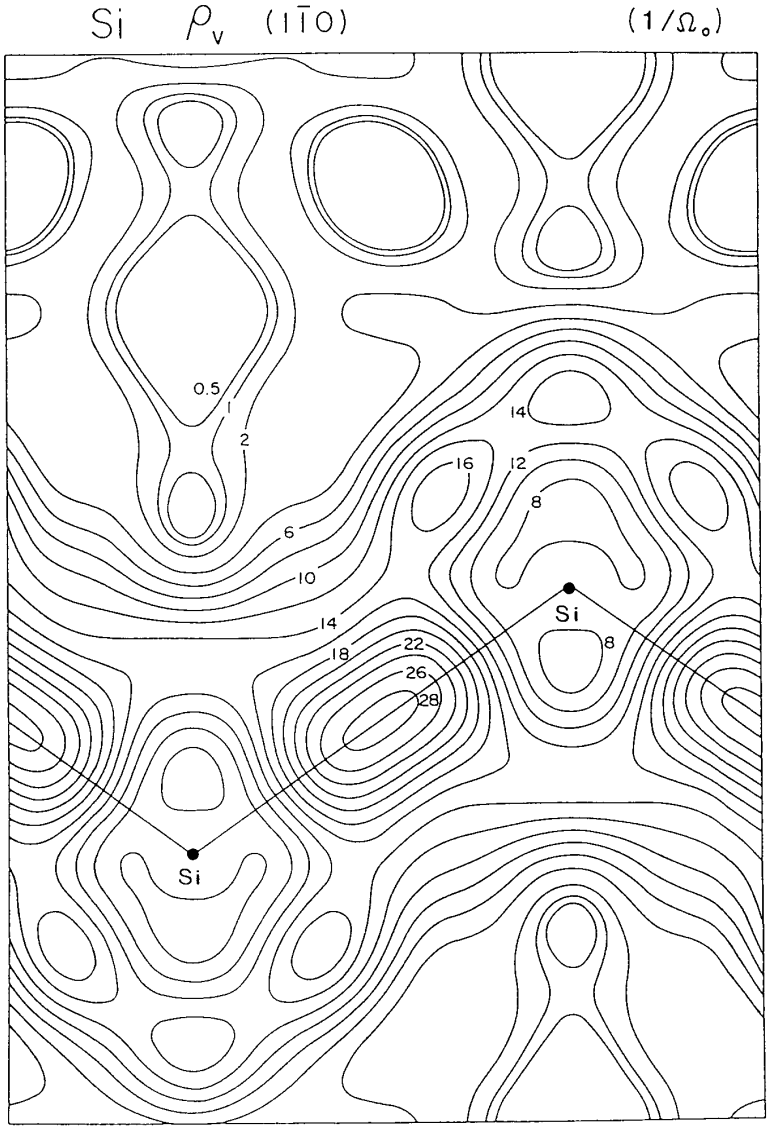

Fig. 6. *Experimental* density of valence electrons of Si in the $(1\bar{1}0)$ plane constructed from the valence electron X-ray structure factors $F_V(\boldsymbol{G})$'s listed in Table III, deduced from the data given in ref. 2, in units of $1/\Omega_0$. This is a corrected map of Yang-Coppens' original[2].

References

1) J.C. Phillips: Chap. 5 Energy Bands in *Bonds and Bands in Semiconductors*, Academic Press, New York and London, 1973, 98-125; Chap. 6 Pseudopotentials and Charge Densities, *ibid.*, 126-153

2) Y.W. Yang and P. Coppens: On the Experimental Electron Distribution in Silicon, Solid State Commun. **15**, 1555-1559, 1974

3) J.R. Chelikowsky and M.L. Cohen: Electronic Structure of Silicon, Phys. Rev. **B10**, 5095-5107, 1974

4) J.P. Walter and M.L. Cohen: Pseudopotential Calculations of Electronic Charge Densities in Seven Semiconductors, Phys. Rev. **B4**, 1877-1892, 1971

5) I.V. Abarenkov and V. Heine: The Model Potential for Positive Ions, Philos. Mag. **12**, 529-537, 1965

6) H. Nara and T. Kobayasi : Nonlocal Pseudopotentials of Si and Ge, J. Phys. Soc. Jpn. **41**, 1429-1430, 1976
7) E. Clementi : *Tables of Atomic Functions*, Suppl. to the paper "Ab Initio Computations in Atoms and Molecules", IBM J. Research and Develop. **9**, 2-19, 1965
8) T. Fukamachi : Mean X-Ray Scattering Factors Calculated from Analytical Roothaan-Hartree-Fock Wave Functions by Clementi, Tech. Rep. of ISSP, University of Tokyo, Ser. **B**, No. 12, 1971
9) J.R. Chelikowsky and M.L. Cohen : Nonlocal Pseudopotential Calculations for the Electronic Structure of Eleven Diamond and Zinc-Blende Semiconductors, Phys. Rev. **B14**, 556-582, 1976